IMPACT INDUCED MOTION OF LARGE BOULDERS AND THEIR EFFECT ON EJECTA EMPLACEMENT ON RUBBLE-PILE TARGETS. J. Ormö[1], S.D. Raducan[2], R. Luther[3], M.I. Herreros[1], M. Jutzi[2], K. Wünnemann[3,4], and G.S. Collins[5]. [1]Centro de Astrobiologia (CAB), CSIC-INTA, Spain (ormoj@cab.inta-csic.es); [2]Space Research and Planetary Sciences, University of Bern, Switzerland; [3]Museum für Naturkunde Berlin, Leibniz Institute for Evolution and Biodiversity Science, Germany; [4]Freie Universität Berlin, Germany; [5]Department of Earth Science Engineering, Imperial College London, UK.

Introduction: Asteroids smaller than about 50 km in diameter are thought to be the result of the break-up of a larger parent body [1]. They are often considered to be "rubble-piles", aggregates held together only by self-gravity and/or small cohesive forces [2, 3]. In 2019, JAXA's Hayabusa2 mission performed an artificial impact experiment by launching the 2 kg Small Carry-on Impactor (SCI), at 2 km/s into the surface of asteroid Ryugu [4]. The impact produced a well-defined crater (~14 m in diameter), despite the presence of large boulders close to the impact point [5]. Images of the SCI impact site before and after impact, revealed that the boulders had different motion mechanisms depending on size and initial position. For example, ~1 m boulders were ejected several metres, a 5 m boulder was moved by about 3 m, while the large, possibly deeply rooted boulder Okamoto was not moved noticeably [4]. However, the final crater morphology appears symmetrical on the side with smaller and mobilised boulders, whereas Okamoto seems to have prevented ejection of finer material.

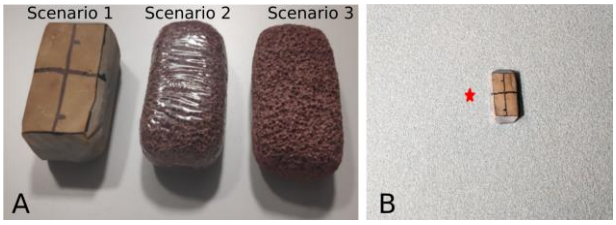

Figure 1. Experiment setup for study of effects of a single large boulder half embedded in the surface of a fine-grained substrate. A) High-density quartzite boulder to the left and low-density pumice boulders to the right. Boulder dimensions are ~ 9x5x3cm³. B) Target set-up with point of impact (red star) at a distance equal to the boulder short axis.

Most previous impact experiments and subsequent validation work of numerical models have focused on homogeneous targets [e.g., 6-8], while recent space missions to asteroids have shown that the asteroid surfaces can be very heterogeneous. Recently, several studies [e.g., 9, 10] have shown that the cratering outcome (i.e., crater and ejecta morphology) depends not only on the material properties, but also on the target structure.

Numerical simulations [11] have reproduced the outcome of the SCI impact with high fidelity. Impact experiments by [12] on granular targets with embedded porous, spherical boulders at velocities of ~400 m/s showed that the impact leads to a displacement of boulders, rather than fragmentation, except for the boulders directly hit by the projectile. Similar results were obtained by [13] for their 5 km/s hypervelocity impact experiments into coarse gravel. However, the sensitivity of the impact cratering outcome (e.g., final crater and ejecta morphology) to the boulders properties (e.g., strength, porosity, size) and distance from the impact location are still not well studied.

Here we combine impact experiments and numerical simulations using shock physics codes to study the cratering outcome and the motion mechanism of large boulders placed close to the impact site (Fig. 1), especially the effect of boulder's bulk density and surface roughness on their mobilisation and ejection, as well as on the excavation flow and ejection of fine-grained matrix. We use the experimental results as constraints for the shock physics codes to validate the numerical 3D results for two end-member cases of boulders with different densities. Then, we expand the parameter space to analyse the transition between these end-member scenarios.

Experimental methods: We performed vertical, half-space impact experiments using the EPIC facility [6], which were recorded by two high-speed cameras. The EPIC utilises a 20 mm calibre compressed N_2 (300 bar) cannon. Here, we launched 20 mm massive, spherical Delrin balls, at 400 m/s. We performed three vertical shots into a loosely packed beach sand in which a single, ~ 9x5x3 cm³ rectangular boulder was embedded to half its thickness (Fig. 1A). In all experiments the point of impact was located as shown in Figure 1B. Coloured sand on the surface allows studies of ejecta distribution.

Scenario 1: The boulder was made of quartzite and had a relatively high bulk density (~ 2.8 g/cm^3).

Scenario 2: The boulder was made of highly porous pumice ((~ 0.27 g/cm^3) with a glossy surface (the boulder was covered in a plastic film).

Scenario 3: The boulder was made of highly porous pumice ((~ 0.27 g/cm^3) with a rough, high-friction surface.

Numerical simulations: Here, we used two shock physics codes: iSALE-3D [14] and Bern SPH [15]. The target is simulated using parameters from [12]. A high-density boulder simulation ("Scenario 1") and a low-density boulder simulation (here called "Scenario 2/3") are made as surface roughness can not be resolved at this resolution. However, the experiments show that surface roughness does not need to be explicitly modelled. The boulders are modelled using a high

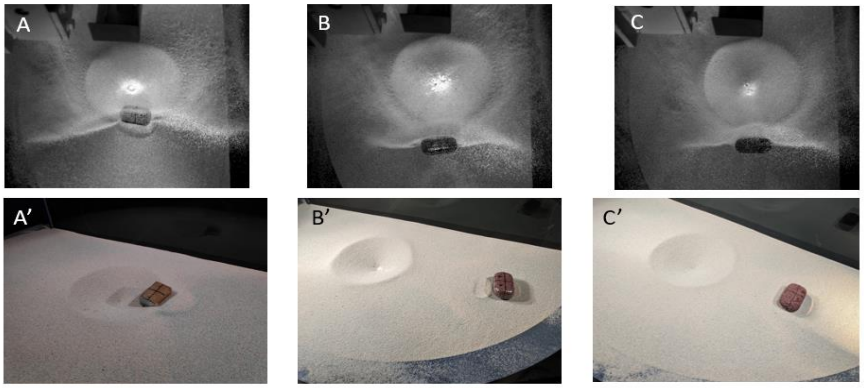

Figure 2. Three experiments with a large boulder partially embedded in a fine-grained substrate. A-C) Vertical view of the effect of the boulder on ejecta emplacement for Scenario 1 (quartzite), Scenario 2 (glossy), and Scenario 3 (rough) respectively at the same time frame. For scale, each boulder is approximately 9cm long. A', B', and C' each show the final crater, ejecta distribution, and the landing site of the respective boulder.

tensile strength that prevents fragmentation, as shown by the experiments.

Results and discussion: We observe a significant difference in the ejection behaviour between the cases with boulders of different density.

In Scenario 1, the boulder was moved a few cm by the excavation flow and deposited at the crater rim. The ejecta curtain passes around the boulder, creating a "forbidden zone" behind the boulder (Fig. 2A). Similar ejecta behaviour was seen during the SCI impact around the Okamoto boulder [4]. On the other hand, in Scenarios 2 and 3, the boulder was excavated with the ejecta curtain, rotated around its length axis ~270° and landing about one crater diameter away from the crater. The ejecta curtain was again obstructed by the presence of the boulder (Fig. 2 B, C). The surface roughness had no obvious effect on boulder movement.

The final rim-diameter of the crater produced in Scenario 1 was ~27 cm , while in Scenarios 2 and 3, it was ~ 29 cm. These results suggest that the presence of a dense (i.e., mainly stationary) boulder close to the impact point does not greatly affect the crater size. However, we can clearly see a significant influence of the boulder on the ejecta curtain behaviour.

The model runs of both iSALE-3D and Bern SPH reveal similar results in terms of crater size and boulder ejection as observed in the experiments. The porous boulder is ejected with the ejecta flow and rotates along its long axis and lands outside the crater, while the dense boulder is only slightly moved outwards to a position on top of the rim, and the sand ejection flow is obstructed (Fig. 3).

The results presented here are important not only in the context of the SCI impact, but they can also be used to understand the cratering mechanisms for NASA's DART impact and other larger natural hypervelocity impacts. However, some relations such as the ratio of impactor size/boulder size need to be scaled to the low-g environment.

Acknowledgements: JO was supported by grant PID2021-125883NB-C22 by the Spanish Ministry of Science and Innovation/State Agency of Research MCIN/AEI/ 10.13039/501100011033. SDR, MJ, RL and KW have received funding from the EU's H2020, grant agreement No. 870377 (NEO-MAPP). SDR and MJ acknowledge support from SNF.

References: [1] Bottke et al. (2005) Icarus, 179: 63–94. [2] Richardson et al. (2002) Asteroids III: 501–515. [3] Scheeres et al. (2010) Icarus, 210, 968. [4] Arakawa et al. (2020), Science, 368, 67. [5] Sakatani et al. (2021) Nature Astro, 5: 766–774. [6] Ormö et al. (2015) Meteorit Planet Sci, 50: 2067-2086. [7] Wünnemann (2016) Meteorit Planet Sci, 51:1762-1794. [8] Luther et al. (2022) Plan.Sci.Jou 3.227. [9] Raducan et al. (2022) A&A, 665, L10. [10] Raducan et al., (2020) Planet Space Sci. 180, 104756. [11] Jutzi et al. (2022) Nature Comm. 13, 7134. [12] Ormö et al. (2022) EPSL, 15, 117713. [13] Housen and Holsapple (2014), LPSC. [14] Wünnemann, K. et al. (2006) Icarus, 180:514–527. [15] Jutzi, M. et al. (2008) Icarus, 198:242–255.

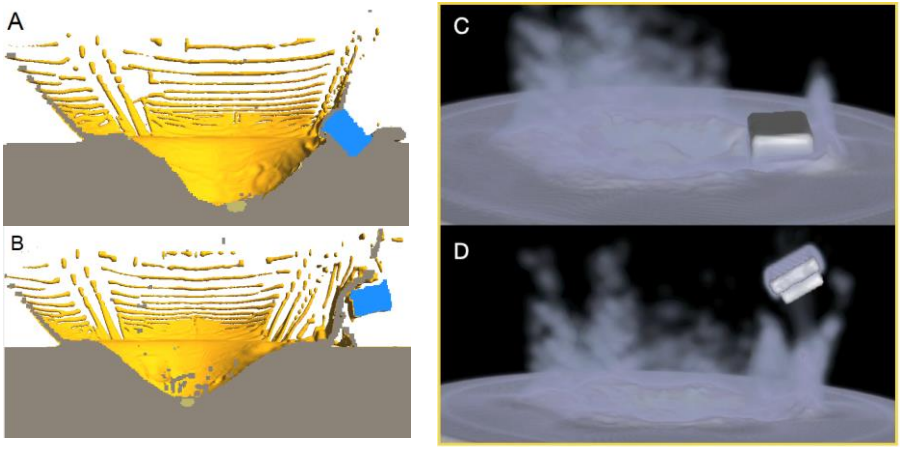

Figure 3. Snapshots from Scenario 1 (A, C) and 2/3 (B, D) after 0.13s simulated with iSALE-3D (A, B) and Bern SPH (C, D). In A and B, blue denotes the boulder, light brown the projectile, and brown the sand material.